

From Polyethylene to Conjugated Polyenes: a Mechanochemical One-Pot Upcycling Strategy for Selective Functionalization

Emna Ben Ayed, Juliette Delcorps, and Olivier Coulembier*

Upcycling strategies for polyolefins remain a significant challenge due to their chemical inertness and complex degradation pathways. A solvent-free, mechanochemical approach is reported to introduce conjugated polyene sequences into polyethylene (PE) via a twin-screw extrusion process. The controlled iodination/elimination strategy enables the stereoselective formation of *cis-transoid* polyenes, a configuration typically achieved under cryogenic conditions but here accessible at high temperatures (106 °C) in a melt-processing environment. This novel approach is confirmed through spectroscopic characterization, including ATR-FTIR, Raman, and CP-MAS ¹³C NMR, and a Diels–Alder reaction that verified the stereochemistry of the resulting polyene. The polymer shows remarkable oxidative stability, with no degradation observed even after six months under ambient conditions. The unsaturated fragments within the polymer exhibit distinct reactivity, allowing selective post-functionalization via epoxidation under reactive extrusion conditions. Mechanochemical epoxidation with *m*-chloroperoxybenzoic acid (*m*CPBA) improves solubility and processability without chain fragmentation, as evidenced by SEC analysis. This work presents a scalable route for the selective functionalization of polyolefins, opening new avenues for their valorization into advanced materials and demonstrating the feasibility of high-temperature processing for the formation of conjugated polyenes.

most problematic plastic uses. A large portion of these plastics ends up in terrestrial and aquatic ecosystems, contributing significantly to greenhouse gas emissions^[3] and exacerbating global warming, posing catastrophic threats to planetary health. Reports have shown that polyethylene is one of the largest emitters of methane and ethylene.^[4] Various approaches to address post-consumer polyolefins, such as mechanical recycling, chemical recycling, and incineration, have been implemented. However, mechanical recycling compromises product quality, chemical recycling produces complex hydrocarbon blends that are difficult to separate, and incineration releases substantial quantities of greenhouse gases.^[5,6] Recovering polymer subunits is also energetically inefficient.^[5]

The concept of “upcycling” has emerged as a promising approach, involving the transformation of post-waste polyolefins into value-added products by introducing active sites into their chemical structures. This process

enables reactions that produce valuable products for further use. One of the most studied processes is dehydrogenation, which weakens the main polymer chains by forming double bonds. Dehydrogenation can be achieved using metallic catalysts, such as iridium complexes,^[7] to introduce unsaturations or serve as an intermediate step for reactions like tandem ethenolysis and isomerization (Iridium complex/*ZnSiO₂*, *Na/γ-Al₂O₃·WO₃/SiO₂*)^[8,9] and cross-alkane metathesis (Ru-based complexes,^[10,11] Iridium complexes^[12]). Additionally, dehydrogenation has been explored for Diels–Alder reactions to produce comonomers and break down high-density polyethylene into telechelic macromonomers for depolymerization and repolymerization.^[13] Despite the potential of these reactions, several challenges hinder their large-scale application. Many catalysts are prohibitively expensive, air-sensitive, and occasionally toxic (especially Ru-based catalysts),^[14] making them impractical for widespread use. Catalyst deactivation is another major limitation, often caused by the reaction duration or the presence of impurities and contaminants in postconsumer plastics.^[10,15] Furthermore, some catalysts require a certain percentage of

1. Introduction

Plastic materials have dominated nearly every aspect of daily life since the 1950s. Their versatility explains their widespread use: they are moldable, dyeable to meet consumer preferences, chemically inert, lightweight, and offer tailored physical and mechanical properties.^[1] These properties have led to their dominance, with global production reaching 413.8 million tons (Mt) in 2023 and projected to exceed 500 Mt by 2050.^[2] Polyolefins account for at least 40% of the plastics consumed worldwide, primarily in short-lived applications like packaging, one of the

E. Ben Ayed, J. Delcorps, O. Coulembier
Laboratory of Polymeric and Composite Materials
University of Mons
Place du Parc 23, Mons 7000, Belgium
E-mail: olivier.coulembier@umons.ac.be

 The ORCID identification number(s) for the author(s) of this article can be found under <https://doi.org/10.1002/adsu.202500571>

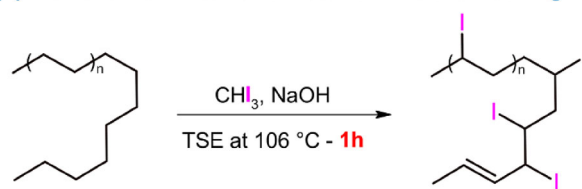
DOI: 10.1002/adsu.202500571

unsaturation to initiate the reaction, adding another layer of complexity.^[16]

In this context, reactive extrusion has emerged as a powerful and scalable platform for polyolefin upcycling, combining mechanical, thermal, and chemical stimuli in a continuous process to selectively functionalize polymer chains while minimizing undesired side reactions.^[17–19] Recent advances demonstrate that radical-based C-H functionalization can be performed directly within twin-screw extruders, enabling the introduction of functional groups that improve polymer adhesion and mechanical properties without compromising polymer integrity.^[19,20] Additionally, reactive extrusion has proven effective in treating mixed or incompatible polyolefin blends, where in situ cross-linking and grafting reactions generate phase-separated nanostructures that enhance ductility, dimensional stability, and recyclability.^[18] Mechanochemical activation under extrusion conditions further allows for the initiation of radical chain reactions under mild, solvent-free conditions with energy efficiency and operational simplicity.^[21,22] These attributes establish reactive extrusion as a key tool in developing innovative, sustainable approaches for polyolefin valorization, motivating its application in the present study.

Recently, we developed a solvent-free, mild-temperature extrusion process that enables the direct iodination of polyolefins using iodoform, CHI_3 , as the iodine source and sodium hydroxide, NaOH , as an initiator.^[23] Operating at low temperature ($106\text{ }^\circ\text{C}$), this method facilitates the efficient functionalization of both polyethylene (PE) and polypropylene (PP), achieving up to 23 wt.% iodine incorporation, without chain cutting, in a kinetically controlled process. Notably, prolonged extrusion led to the formation of few in-chain $\text{C}=\text{C}$ bonds, as demonstrated by various spectroscopic and thermal techniques. The extent of these unsaturations was found to correlate with both the initiator content and the applied shear forces, ultimately influencing the polymer solubility and reactivity. Recent investigations on a model n -hexadecane (n -C16) molecule, easy to characterize by NMR spectroscopy, revealed that although iodination proceeded efficiently at the onset of the reaction, the iodine conversion unexpectedly declined after extended reaction times. For instance, under reaction conditions with a $[\text{n-C16}]_0/[\text{CHI}_3]_0/[\text{NaOH}]_0$ ratio of 1/1/1 at $106\text{ }^\circ\text{C}$, proton nuclear magnetic resonance (^1H NMR) spectroscopy showed that after 2 h, one iodine atom was incorporated per four n -C16 chains, while one chain out of 200 carried a carbon-carbon double bond. After 144 h of reaction, however, the iodination decreased, with one iodine atom incorporated per six chains and one chain out of eight exhibiting a double bond (Figures S1 and S2, Supporting Information). This basic model indicated a dynamic interplay between iodination and elimination reactions, even under conditions not optimized for efficient elimination. Initially, CHI_3 and NaOH promoted iodination, but beyond a certain threshold, NaOH started acting as a base, inducing elimination and leading to the formation of unsaturated species. Unlike conventional dehydrogenation methods that require costly, air-sensitive metal catalysts, this transformation occurred under simple, metal-free conditions using NaOH – a widely available and inexpensive base – without the need for solvents or complex reaction setups. These advantages have motivated us to further explore this process to assess its potential as a scalable and cost-effective method for introducing

(A) Previous work: iodination reaction – no chain cutting



(B) This work: unsaturation process – no chain cutting

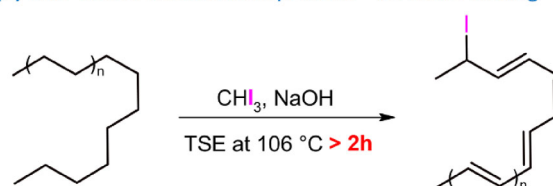


Figure 1. Iodination versus elimination: tuning polyolefin reactivity under mild extrusion conditions. A) Previously developed solvent-free iodination of polyethylene using CHI_3 and NaOH , leading to well-defined iodinated polymers.^[23] B) This work: controlled shear-induced elimination promotes the formation of polyolefins with multiple unsaturations while retaining residual iodine functionalities. TSE: Twin-screw extrusion.

double bonds into polyolefins under mild extrusion conditions (Figure 1).

Beyond its chemical innovation, this work contributes to the United Nations Sustainable Development Goals, particularly SDG 12 (Responsible Consumption and Production), by proposing a scalable and solvent-free upcycling strategy for polyolefins. It opens new avenues for converting plastic waste into higher-value functional materials, offering a more circular and sustainable approach to plastic use.

2. Results and Discussion

To further investigate the influence of reaction parameters on the balance between iodination and elimination, the proportion of elimination reactions was enhanced by increasing shear force and reaction time while maintaining a minimal NaOH concentration. Although NaOH is a widely available and inexpensive base, its excessive use was avoided to limit unnecessary side effects. Instead, two samples were prepared under medium to high shear conditions (screw speed, SS, of 200 to 300 rpm), with reaction times of 2 h (PE_1) and 5 h (PE_2) for an initial $[\text{C}_2\text{H}_4]_0/[\text{CHI}_3]_0/[\text{NaOH}]_0$ of 1. To facilitate processing and to enable precise structural modifications, the study was conducted on a low-molecular-weight linear low-density polyethylene (LLDPE; theoretical $M_w \approx 1500\text{ g mol}^{-1}$). This model system provides a controlled platform to probe chemical reactivity under mild conditions, with potential for extension to postconsumer polyolefin waste streams, including low-density polyethylene (LDPE). LDPE is widely used in packaging materials such as films and plastic bags, yet often regarded as challenging to recycle due to its low density and branched structure. Nevertheless, LDPE represents a significant portion of global plastic waste and is actively targeted in mechanical and chemical recycling schemes. In Belgium alone, plastic packaging waste accounts for ≈ 366000 tons annually, with LDPE films constituting a major fraction.^[24]

Encouragingly, Belgium ranks among the top EU performers in plastic recycling, with packaging plastics recycled at a rate of 54% in 2022 – up from 29% in 2002.^[25] This improvement is largely attributed to the implementation of inclusive collection systems (e.g., the “New Blue Bag” scheme) that now encompass flexible LDPE-based materials.^[26] Several industrial initiatives illustrate the strategic importance of LDPE recycling. For instance, Raff Plastics (Londerzeel) specializes in recycling industrial LDPE waste into high-quality compounds for construction and manufacturing.^[27] Phoenix Plus SA handles post-consumer LDPE along with other polyolefins, transforming waste into reusable feedstocks for international markets.^[28] In Beringen, Chiro has developed advanced AI-based sorting lines specifically tailored for LDPE films, producing recycled materials of commercial quality.^[29]

These examples underscore the relevance of LDPE as a recyclable polyolefin. In line with this, we have previously demonstrated that our iodination procedure – applied to isotactic polypropylene at 106 °C, ca. 30 °C below its melting point – allowed successful functionalization without chain scission.^[23] This supports the generalizability of our method to chemically modify polyolefin waste streams, including LDPE, under industrially relevant conditions. To evaluate the practical feasibility of such modifications, we revisited our iodination/elimination protocol under controlled conditions. Previous studies had already demonstrated that 2 h of reaction led to PE modified with 15 wt.% iodine, while also exhibiting a significant degree of unsaturation, as attested by the appearance of a charring plateau \approx 19 wt.% during thermogravimetric analysis (TGA).^[23] Extending the reaction time to 5 h allowed a deeper assessment of the impact of prolonged extrusion on the competition between iodination and elimination. For PE₂, a 9 wt.% iodine loss and a charring plateau of 32 wt.% were observed (Figure S3, Supporting Information), providing additional insight into the dynamics of iodination and elimination under these conditions, thus reinforcing the understanding of the reaction balance under mild yet mechanically intense conditions. The moderated solubility of PE₁ and the full insolubility of PE₂ prevented direct comparison by ¹H NMR spectroscopy. A differential scanning calorimetry (DSC) study was used to observe the impact of the degree of unsaturation on the thermal behavior of the samples, as it does not directly quantify carbon-carbon double bonds. Compared to pristine PE (melting temperature, $T_m = 105$ °C and crystallinity, $\Delta\chi = 21\%$), PE₁ exhibited a lower melting point (83 °C, $\Delta\chi = 7\%$), while PE₂ displayed an even more pronounced decrease (66.3 °C, $\Delta\chi = 3\%$) (Figure S4, Supporting Information). This progressive loss of crystallinity with increasing reaction time under high shear conditions strongly suggests that elimination reactions disrupt the polymer-ordered domains, leading to a higher incorporation of unsaturations within the polymer matrix.

To gain further insights into the nature of the unsaturations, attenuated total reflectance Fourier-transform infrared (ATR-FTIR) spectroscopy was employed to analyze the molecular structures of iodinated polyethylene samples (PE₁ and PE₂) in comparison with pristine PE. The spectrum of pristine PE exhibited four distinct absorption bands at 2918, 2850, 1465, and 721 cm⁻¹, corresponding to CH₂ asymmetric stretching, CH₂ symmetric stretching, CH₂ bending vibrations, and CH₂ rocking motions, respectively.^[30] In contrast, the spectra of PE₁ and

PE₂ showed a broader CH₂ bending peak centered at 1463 cm⁻¹, suggesting alterations in the local molecular environment due to iodination.^[31] Moreover, new absorption bands emerged at \approx 1330 and 779 cm⁻¹, attributable to CH₃ deformation modes. Particularly noteworthy were the broad absorption features observed in 1645–1569 cm⁻¹ region, characteristic of C=C stretching vibrations, along with a distinct band at 779 cm⁻¹, indicative of =C–H bending modes associated with the *cis* isomer of internal alkenes (Figure 2A).^[32] Interestingly, this observation contrasts with the recent work by Abu-Omar et al.,^[33] where the elimination of bromine halogen atoms led to the preferential formation of *trans*-internal alkenes, the thermodynamically more stable isomer.^[34] Additionally, the stretching mode peak shifted to higher frequencies, suggesting the presence of conjugated double bonds and polyene sequences,^[35,36] a hypothesis requiring further spectroscopic confirmation. Notably, no oxidation of the double bonds was detected, as evidenced by the absence of a peak at 1710 cm⁻¹ associated with carbonyl groups.^[24] To confirm the conjugation hypothesis inferred from FTIR analysis, Raman spectroscopy was performed using an excitation wavelength of 523 nm. For PE₁, a strong peak was observed at 1589 cm⁻¹, assigned to the C=C stretching mode within a conjugated system, specifically a *cis-transoid* isomer configuration.^[37,38] As depicted in Figure 2B, a secondary peak merges with the primary peak, forming an intermediate frequency. Previous studies on short conjugated systems have attributed such behavior to coupling between the C–C and C=C stretching modes, a phenomenon characteristic of relatively short polyene sequences.^[39] In contrast, no significant Raman signal was detected for PE₂, even at a higher excitation wavelength of 783 nm, suggesting that extensive structural modifications hinder effective resonance enhancement.

Further insights into the nature of these polyenes were obtained via solid-state cross-polarization magic-angle spinning (CP-MAS) ¹³C NMR spectroscopy (Figure 2C). The PE₁ and PE₂-based spectra displayed a broad peak \approx $\delta = 100$ ppm, confirming the presence of the *cis*-isomer previously identified by FTIR and Raman spectroscopy. Interestingly, the observed chemical shifts appeared at lower frequencies than those typically reported for conjugated polyenes,^[40,41] likely due to the influence of iodine atoms. While iodine introduces polarity, it may also disrupt conjugation, affecting the electronic environment and spectral characteristics.^[42] Additionally, factors such as polyene chain length, bond alternation, and angular strain further modulate the chemical shifts.^[43]

The CP-MAS ¹³C NMR spectrum also provided insights into the polymer crystallinity: increasing structural disorder following functionalization resulted in a shift in the methylene peak. For PE₁, two signals were observed at $\delta = 32.64$ ppm and $\delta = 31.15$ ppm, while for PE₂, the signal at $\delta = 31.15$ ppm became predominant. These shifts support a reduction in crystallinity, with the signal at $\delta = 32.64$ ppm typically assigned to the crystalline phase and the one at $\delta = 31.15$ ppm associated with the amorphous region.^[44,45] This shift is consistent with the increasing disruption of the polymer-ordered structure with prolonged reaction time, in accord with the DSC data.

To the best of our knowledge, only a very limited number of studies have reported [4 + 2] Diels–Alder reactions involving polyacetylene or even its oligomeric forms.^[46,47] This scarce reactivity is likely due to the intrinsic properties of such systems,

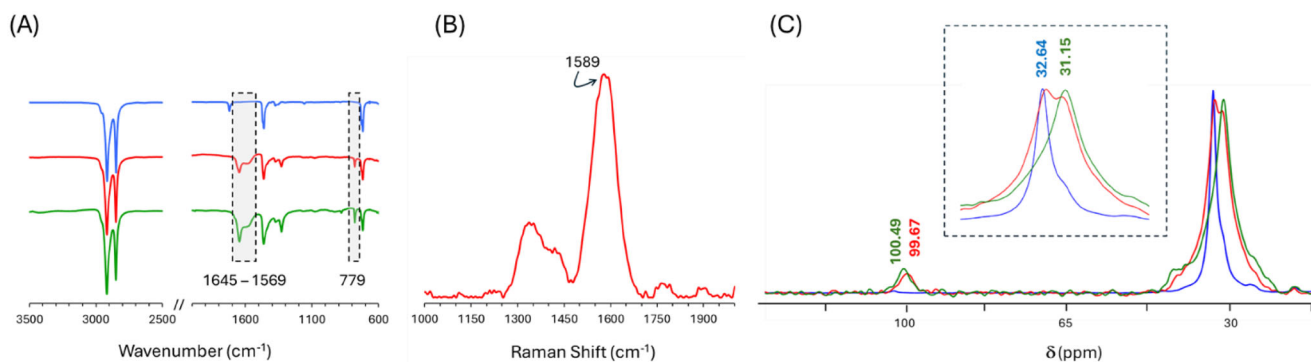
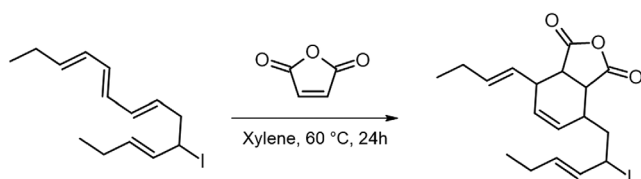


Figure 2. A) ATR-FTIR spectra of pristine PE (blue), PE₁ (red), and PE₂ (green), highlighting the appearance of C=C stretching vibrations and =C–H bending modes, indicative of unsaturation. B) Raman spectrum of PE₁ at an excitation wavelength of 523 nm, revealing a prominent peak at 1589 cm⁻¹ associated with conjugated double bonds. C) CP-MAS ¹³C NMR spectra of pristine PE (blue), PE₁ (red), and PE₂ (green), showing a broad resonance $\approx \delta = 100$ ppm, further supporting the presence of unsaturated structures.

including their predominant *trans* configuration, extended conjugation length, and limited solubility. However, gathered spectroscopic data suggest the presence of short conjugated sequences in a *cis-transoid* conformation, along with iodine atoms covalently bound to the polymer backbone. These structural features may facilitate the [4+2] cycloaddition reaction by modulating the electronic environment of the diene units. To explore this reactivity, a model Diels–Alder reaction was performed between our polymer and maleic anhydride (MA). Given its superior solubility, PE₁ was selected as the substrate, and the reaction was carried out in xylene at 60 °C for 24 h (Scheme 1).

After purification, ¹H NMR analysis revealed the formation of a new functional group, with a signal at $\delta = 3.74$ ppm, attributed to the methine protons in α position to the carbonyl groups of the generated tetrahydrophthalic anhydride unit (Figure 3). Notably, no vinyl signals corresponding to newly formed C=C bonds were detected, consistent with their absence in unreacted PE₁. This absence is likely due to their restricted mobility in solution.^[23] Interestingly, the signal assigned to the iodine-linked methine proton before the reaction remained unchanged at $\delta = 4.11$ ppm, confirming both the retention of iodine within the polymer structure and the non-radical nature of the Diels–Alder reaction. These results provide clear evidence of conjugated diene segments within the modified PE structure, suggesting that polyethylene derivatives adopt a conformation favorable to the Diels–Alder reaction. Furthermore, the carbonyl stretching vibration at ≈ 1710 cm⁻¹ in the FTIR spectrum (Figure S5, Supporting Information) further corroborates the successful functionalization.



Scheme 1. Diels–Alder reaction between a modified polyethylene fragment bearing supposed conjugated double bonds in a *cis-transoid* configuration and iodine atoms, and maleic anhydride, conducted in xylene at 60 °C for 24 h.

The formation of conjugated polyene sequences under these reaction conditions suggests an elimination pathway distinct from classical dehydrohalogenation observed in polyhalogenated polymers such as poly(vinyl chloride) (PVC), where base-induced elimination predominantly yields *trans* polyenes.^[41] In PVC, dehydrohalogenation typically follows a well-established mechanism, where the elimination of chlorine leads to the formation of thermodynamically stable *trans*-configured alkenes.

In contrast, the system presented here, involving PE, operates under conditions that induce localized iodination followed by dehydroiodination, leading to the formation of conjugated polyene sequences in a *cis-transoid* conformation. To our opinion, the key to this process lies in the precise positioning of iodine atoms within the polymer backbone, which plays a critical role in stabilizing the intermediate structure (Step 1) before elimination occurs (Step 2). Once iodine atoms are positioned, base-induced elimination, following a favorable E2 mechanism, takes place. In this process, a proton is eliminated in an anti-periplanar configuration relative to the iodine atom, promoting the formation of

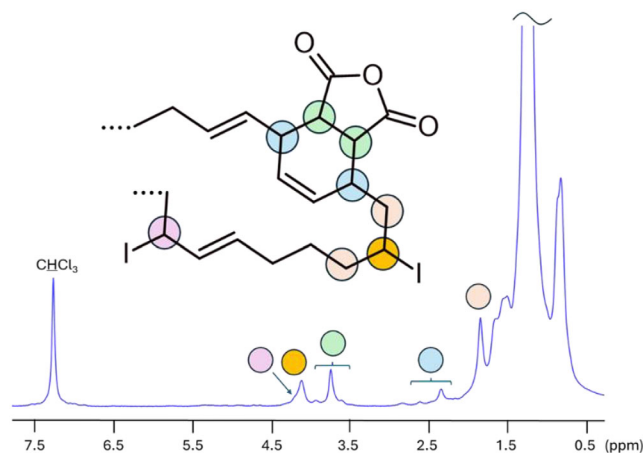
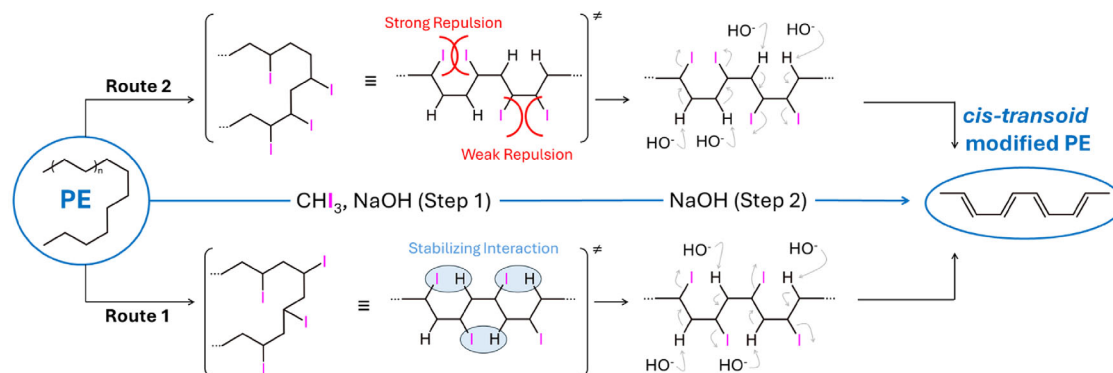


Figure 3. ¹H NMR spectrum (500 MHz, 21 °C, CDCl₃) of modified PE₁ after the Diels–Alder reaction with MA. Colored dots indicate the most relevant proton signals.



Scheme 2. Proposed pathways for *cis-transoid* polyene formation: Route 1 stabilizes iodine positioning on alternating methylene units, while Route 2 involves adjacent iodine atoms, leading to a less stable intermediate.

conjugated polyene sequences. The shear force and temperature during the extrusion process increase the degrees of freedom in the polymer chains, favoring the alignment of hydrogen atoms in the anti-position with respect to iodine atoms, thereby facilitating the elimination process.

This dynamic system maintains a balance between iodination and elimination, with the final product predominantly governed by reaction time and shear force. For the formation of *cis-transoid* isomers, two potential iodine positioning modes can be considered. In the first scenario, iodine atoms are positioned on a carbon flanked by two methylene units (Route 1, **Scheme 2**), thereby interacting with neighboring protons through halogen bonding, which stabilizes the structure and promotes elimination. In the second scenario, iodine atoms are placed on α and β adjacent carbon atoms, twisted between ethylene and methylene units (Route 2, **Scheme 2**), leading to a less stable intermediate, where steric hindrance and electronic effects from the neighboring iodine atoms reduce stability. The favorable iodine–hydrogen interaction in the first scenario enhances the stability of the intermediate structure, favoring the E2 elimination mechanism and driving the formation of conjugated polyenes.

Remarkably, our conditions enable the selective formation of short-length conjugated polyenes predominantly in the less thermodynamically stable *cis-transoid* isomer, a configuration typically accessible only through cryogenic routes (e.g., $-78\text{ }^{\circ}\text{C}$) followed by thermal isomerization to the more stable *trans* form.^[48,49] In stark contrast, our mechanochemical approach achieves this uncommon isomer directly at $106\text{ }^{\circ}\text{C}$ in a melt-processing environment – conditions compatible with industrial extrusion. This unprecedented access to *cis-transoid* polyenes under scalable conditions constitutes a significant departure from traditional synthetic routes. Although rarely explored, the *cis-transoid* configuration holds substantial promise: upon doping, it has exhibited electrical conductivities comparable to or even surpassing those of the *trans* isomer.^[50] Moreover, its integration into optoelectronic^[51] and photovoltaic devices, including LED systems,^[52] has recently garnered attention. In our study, no measurable electrical conductivity could be detected by conductive atomic force microscopy (c-AFM), and thermal isomerization to the *trans* form – as described in previous reports – proved unsuccessful. These results indicate that the *cis-transoid* architecture remains kinetically stabilized under our conditions, offering

a unique opportunity to explore structure–property relationships beyond the thermodynamic landscape typically accessed in conjugated polymer chemistry.

Given these observations, the focus shifted toward leveraging the intrinsic reactivity of the conjugated sequences for further functionalization. Since extended conjugation, as in a *trans-transoid* arrangement, disfavors post-functionalization due to the disruption of electronic delocalization, the *cis-transoid* configuration of modified PE may offer greater susceptibility to chemical modification. To probe this potential reactivity, an in situ mechanochemical epoxidation was carried out using *m*-chloroperoxybenzoic acid (*m*CPBA) (**Figure 4**). The incorporation of epoxide groups is particularly advantageous, as it addresses common limitations of polyolefins, such as poor adhesion, low surface energy, and limited chemical reactivity, thereby broadening their potential applications.

To complement the results obtained with PE₁, PE₂ was selected for the epoxidation reaction due to its suspected higher content of olefinic moieties. As previously noted, PE₂ exhibited significant resistance to solubilization in various organic solvents. This insolubility is attributed to the polyene nature of the material, which likely complicates processing. To overcome this limitation, the epoxidation reaction was conducted in bulk through reactive extrusion (SS = 50 rpm) at $50\text{ }^{\circ}\text{C}$, slightly below the polymer T_m . Interestingly, after a few minutes of reaction with an excess of *m*CPBA, the shear forces between the extruder screws gradually decreased, ultimately yielding an off-white solid after 3 h under nitrogen. Following purification, the epoxidized PE₂ (e-PE₂) exhibited enhanced solubility in organic solvents, such as DMSO,

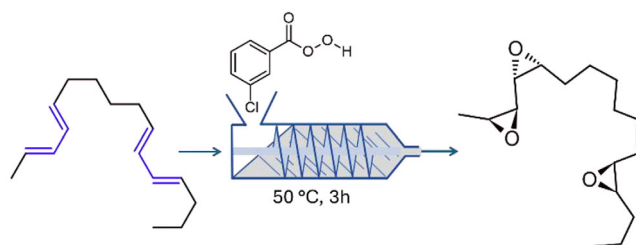


Figure 4. Mechanochemical epoxidation of a *cis-transoid* segment of a modified PE using *m*CPBA under reactive extrusion at $50\text{ }^{\circ}\text{C}$.

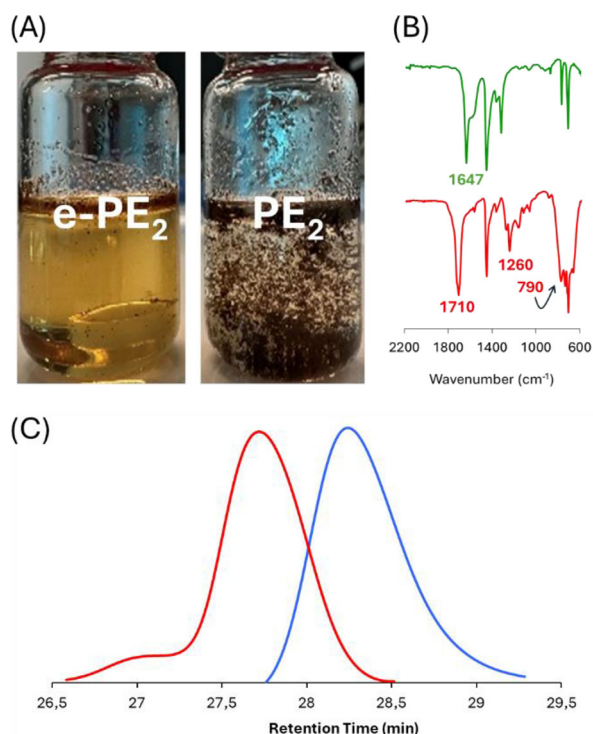


Figure 5. A) Solubility comparison of PE₂ (right) and e-PE₂ (left) in DMSO at 80 °C for 15 h. B) ATR-FTIR spectra of PE₂ and e-PE₂. C) SEC traces of pristine PE (blue) and e-PE₂ (red) recorded in DMSO at 50 °C.

compared to pristine PE₂ (Figure 5A). Notably, even after 15 h at 80 °C, PE₂ remained largely insoluble in DMSO, whereas e-PE₂ showed significantly improved solubility. This suggests that epoxidation effectively disrupts intermolecular interactions and facilitates dissolution.^[53,54] Importantly, the solubilization of e-PE₂ was not due to chain fragmentation, as Size-Exclusion Chromatography (SEC) analysis (Figure 5C) revealed a shift to lower elution volume compared to pristine PE, further supporting the notion that the epoxidation of PE₂ did not lead to chain degradation.

In the epoxidized sample, the presence of an undissolved fraction (Figure 5A, left) was attributed to incomplete conversion of double bonds or a possible formation of higher-molecular-weight species, as evidenced by the SEC data (Figure 5C), which shows a shoulder at lower elution volumes. This hypothesis is partially supported by the FTIR spectra (Figure 5B), where, despite the disappearance of the major peaks associated with carbon-carbon double bond stretching ($\approx 1647\text{ cm}^{-1}$), a low-intensity tailing is still observed between 1672 and 1564 cm^{-1} . Interestingly, the epoxidation process resulted in the formation of oxirane groups, as indicated by new peaks at 790 and 1260 cm^{-1} , corresponding to the C—O—C stretching modes of epoxy groups. The low-temperature solid-state mechanochemical epoxidation conditions favored the integration of oxirane groups into the unsaturated polyethylene chains, although ring-opening reactions may have led to the formation of additional functional groups, such as ketones and carboxylic acids, as suggested by the carbonyl stretching peak at 1710 cm^{-1} .

3. Conclusion

A solvent-free and scalable approach for the selective functionalization of polyethylene has been established through a twin-screw extrusion process, enabling the formation of conjugated polyene sequences in a stereoselective *cis-transoid* configuration. This structure, typically accessible only under cryogenic conditions, was obtained here at $106\text{ }^{\circ}\text{C}$ under mild yet mechanically intense processing, underscoring the potential of extrusion as a tool for polyolefin transformation. The resulting polyene sequences were shown to be chemically addressable, as demonstrated by successful Diels–Alder and epoxidation reactions, thereby expanding the range of post-functionalization strategies applicable to polyolefins. While the methodology was developed using a low-molecular-weight linear PE as a model system, it is designed with scalability and transposability in mind, particularly toward challenging waste streams such as low-density polyethylene (LDPE). Given the relevance of LDPE in packaging and its growing importance in recycling infrastructures, the present strategy contributes to the development of viable chemical upcycling routes for polyolefin-rich waste.

Supporting Information

Supporting Information is available from the Wiley Online Library or from the author.

Acknowledgements

E.B.A. and J.D. gratefully acknowledge the AXA Research Fund for supporting their postdoctoral and predoctoral fellowships, respectively. O.C. acknowledges funding from the F.R.S.-FNRS of Belgium for his position as a Senior Research Associate, as well as support from the AXA Research Fund as an AXA Professor in Chemistry. The authors also thank Prof. Philippe Leclère (University of Mons, Belgium) for his assistance with electrical conductivity measurements and Prof. Christophe Detrembleur (University of Liège, Belgium) for his contribution to the Cross-Polarization Magic Angle Spinning ¹³C NMR spectroscopy analysis.

Conflict of Interest

The authors declare no conflict of interest.

Data Availability Statement

The data that support the findings of this study are available in the supplementary material of this article.

Keywords

conjugated polyene, dehydrogenation, plastic upcycling, polyethylene, twin-screw extrusion

Received: May 7, 2025
Revised: May 29, 2025
Published online:

- [1] J. R. Jambeck, I. Walker-Franklin, *One Earth* **2023**, 6, 600.
- [2] PlasticsEurope, <https://PlasticsEurope.Org/Knowledge-Hub/Plastics-the-Fast-Facts-2024/>, (accessed: August 2024).
- [3] S. R. Nicholson, N. A. Rorrer, A. C. Carpenter, G. T. Beckham, *Joule* **2021**, 5, 673.
- [4] R. Geyer, J. R. Jambeck, K. L. Law, *Sci. Adv.* **2017**, 3, 1700782.
- [5] A. Rahimi, J. M. García, *Nat. Rev. Chem.* **2017**, 1, 0046.
- [6] M. Shen, W. Huang, M. Chen, B. Song, G. Zeng, Y. Zhang, *J. Cleaner Prod.* **2020**, 254, 120138.
- [7] A. Ray, K. Zhu, Y. V. KISSIN, A. E. Cherian, G. W. Coates, A. S. Goldman, *Chem. Commun.* **2005**, 3388.
- [8] R. J. Conk, S. Hanna, J. X. Shi, J. Yang, N. R. Ciccina, L. Qi, B. J. Bloomer, S. Heuvel, T. Wills, J. Su, A. T. Bell, J. F. Hartwig, *Science* **2022**, 377, 1561.
- [9] R. J. Conk, J. F. Stahler, J. X. Shi, J. Yang, N. G. Lefton, J. N. Brunn, A. T. Bell, J. F. Hartwig, *Science* **2024**, 385, 1322.
- [10] N. M. Wang, G. Strong, V. DaSilva, L. Gao, R. Huacuja, I. A. Konstantinov, M. S. Rosen, A. J. Nett, S. Ewart, R. Geyer, S. L. Scott, D. Guironnet, *J. Am. Chem. Soc.* **2022**, 144, 18526.
- [11] M. Nagyházi, Á. Lukács, G. Turczel, J. Hancsók, J. Valyon, A. Bényei, S. Kéki, R. Tuba, *Angew. Chem., Int. Ed.* **2022**, 61, 202204413.
- [12] A. Arroyave, S. Cui, J. C. Lopez, A. L. Kocen, A. M. LaPointe, M. Delferro, G. W. Coates, *J. Am. Chem. Soc.* **2022**, 144, 23280.
- [13] S. M. Parke, J. C. Lopez, S. Cui, A. M. LaPointe, G. W. Coates, *Angew. Chem., Int. Ed.* **2023**, 62, 202301927.
- [14] Y. Kratish, J. Li, S. Liu, Y. Gao, T. J. Marks, *Angew. Chem.* **2020**, 132, 20029.
- [15] P. F. Britt, G. W. Coates, K. I. Winey, J. Byers, E. Chen, B. Coughlin, C. Ellison, J. Garcia, A. Goldman, J. Guzman, J. Hartwig, B. Helms, G. Huber, C. Jenks, J. Martin, M. McCann, S. Miller, H. O'Neill, A. Sadow, S. Scott, L. Sita, D. Vlachos, R. Waymouth, *Rep. Basic Energy Sci. Roundt. Chem. Upcycl. Polym.* **2019**.
- [16] P. A. Kots, *Chem. Catal.* **2024**, 4, 101194.
- [17] J. B. Williamson, C. G. Na, R. R. JonhsonIII, W. F. M. Daniel, E. J. Alexanian, F. A. Leibfarth, *J. Am. Chem. Soc.* **2019**, 141, 12815.
- [18] T. Vialon, H. Sun, G. J. M. Formon, P. Galanopoulou, C. Guibert, F. Averseng, M.-N. Rager, A. Percot, Y. Guillaneuf, N. J. Van Zee, R. Nicolaÿ, *J. Am. Chem. Soc.* **2024**, 146, 2673.
- [19] M. Hua, Z. Peng, R. D. Guha, X. Ruan, K. C. Ng, J. Demarteau, S. Haber, S. N. Fricke, J. A. Reimer, M. B. Salmeron, K. A. Persson, C. Wang, B. A. Helms, *Sci. Adv.* **2024**, 10, adq3801.
- [20] T. J. Fazekas, J. W. Alty, E. K. Neidhart, A. S. Miller, F. A. Leibarth, E. J. Alexanian, *Science* **2022**, 375, 545.
- [21] J. Zhou, T.-G. Hsu, J. Wang, *Angew. Chem., Int. Ed.* **2023**, 62, 202300768.
- [22] K. Kubota, J. Jiang, Y. Kamakura, R. Hisazumi, T. Endo, D. Miura, S. Kubo, S. Maeda, H. Ito, *J. Am. Chem. Soc.* **2024**, 146, 1062.
- [23] E. Ben Ayed, J. Delcorps, O. Coulembier, *Ind. Eng. Chem. Res.* **2024**, 63, 21455.
- [24] Statbel, Packaging Waste, can be found under <https://statbel.fgov.be/en/themes/environment/waste-and-pollution/packaging-waste> (accessed: April, 2025).
- [25] The Brussels Times, "Belgium among the top EU nations for recycling plastic packaging", <https://www.brusselstimes.com/eu-affairs/1284000/belgium-one-of-the-eus-best-performers-for-recycling-plastic-packaging> (accessed: April 2025).
- [26] F. Plus, "Belgium exceeds European plastic recycling requirements", <https://www.fostplus.be/en/blog/belgium-exceeds-european-plastic-recycling-requirements> (accessed: April 2025).
- [27] R. Plastics, "Our Services", <https://www.raffplastics.be/en/our-services> (accessed: April 2025).
- [28] Phoenix Plus SA, "Recycling Solutions", <https://www.phoenixplus.be/en/recycling-solutions> (accessed: April 2025).
- [29] Chiro Beringen, "Innovative Recycling Technologies", <https://www.chiroberingen.be/en/innovative-recycling-technologies> (accessed: April 2025).
- [30] M. A. Smook, E. T. Pieski, C. F. Hammer, *Ind. Eng. Chem.* **1953**, 45, 2731.
- [31] K. Nambu, *J. Appl. Polym. Sci.* **1960**, 4, 69.
- [32] J. Coates, *Encyclopedia of Analytical Chemistry*, (Ed.: R. A. Meyers), Wiley, Hoboken, NJ, USA **2000**.
- [33] M. Zeng, Y.-H. Lee, G. Strong, A. M. LaPointe, A. L. Kocen, Z. Qu, G. W. Coates, S. L. Scott, M. M. Abu-Omar, *ACS Sustain. Chem. Eng.* **2021**, 9, 13926.
- [34] D. James, C. W. Chien, *Polyacetylene: Chemistry, Physics, and Material Science*, Elsevier, Amsterdam, New York **2012**.
- [35] H. Shirakawa, S. Ikeda, *Polym. J.* **1971**, 2, 231.
- [36] A. J. Dias, T. J. McCarthy, *Macromolecules* **1985**, 18, 869.
- [37] L. Dai, *Macromol. Chem. Phys.* **1997**, 198, 1723.
- [38] H. Shirakawa, T. Ito, S. Ikeda, *Polym. J.* **1973**, 4, 460.
- [39] R. L. Christensen, E. A. Barney, R. D. Broene, M. G. I. Galinato, H. A. Frank, *Arch. Biochem. Biophys.* **2004**, 430, 30.
- [40] T. C. Clarke, J. C. Scott, *Solid State Commun.* **1982**, 41, 389.
- [41] J. Wu, K. G. Papanikolaou, F. Cheng, B. Addison, A. A. Cuthbertson, M. Mavrikakis, G. W. Huber, *ACS Sustain. Chem. Eng.* **2024**, 12, 7402.
- [42] T. Yamanobe, I. Ando, *J. Chem. Phys.* **1985**, 83, 3154.
- [43] H. W. Gibson, J. M. Pochan, S. Kaplan, *J. Am. Chem. Soc.* **1981**, 103, 4619.
- [44] N. Chaikut, T. Amornsakchai, H. Kaji, F. Horii, *Polymer* **2006**, 47, 2470.
- [45] R. A. Assink, M. Celina, K. T. Gillen, R. L. Clough, T. M. Alam, *Polym. Degrad. Stab.* **2001**, 73, 355.
- [46] R. Cosmo, H. Naarmann, *Mol. Cryst. Liq. Cryst. Incorporating Nonlinear Opt.* **1990**, 185, 89.
- [47] I. C. McNeill, M. H. Mohammed, E. Y. Davydov, G. E. Zaikov, *Polym. Degrad. Stab.* **1997**, 58, 61.
- [48] H. Shirakawa, E. J. Louis, A. G. MacDiarmid, C. K. Chiang, A. J. Heeger, *J. Chem. Soc., Chem. Commun.* **1977**, 578.
- [49] M. Goh, G. Piao, M. Kyotani, K. Akagi, *Macromolecules* **2009**, 42, 8590.
- [50] T. Yamabe, K. Tanaka, H. Terama-e, K. Fukui, A. Imamura, H. Shirakawa, S. Ikeda, *Solid State Commun.* **1979**, 29, 329.
- [51] S. Wang, X. Sun, H. Zeng, S. Xie, J. Zhang, X. Wan, *Macromolecules* **2025**, 58, 1235.
- [52] K. N. Keya, M. A. Jabed, W. Xia, D. Kilin, P. C.-P. S. Material, *Appl. Sci.* **2022**, 12, 2830.
- [53] X. Jian, A. S. Hay, *J. Polym. Sci., C: Polym. Lett.* **1990**, 28, 285.
- [54] Q. Xiong, S. Yang, C. Peng, F. Xie, Z. Gu, Y. Fu, H. Tan, Q. Dai, W. Yi, L. Li, K. Liu, *J. Polym. Res.* **2023**, 30, 326.